DOI: 10.1002/ejic.200900685

Syntheses, Crystal Structures and Mass Spectrometry of Mononuclear Ni^{II} Inclusion Product and Self-Assembled [2 × 1+1 × 2] $Ni^{II}_3M^{II}$ (M = Cu, Ni, Co, Fe or Mn) Cocrystals Derived from *N*,*N'*-Ethylenebis(3-ethoxysalicylaldimine)

Sohini Sarkar,[a] Malabika Nayak,[a] Michel Fleck,[b] Supriya Dutta,[c] Ulrich Flörke,[d] Rajesh Koner,*[a] and Sasankasekhar Mohanta*[a]

Keywords: Hydrogen bonds / Self-assembly / Mass spectrometry / Inclusion compounds / Crystal engineering

The syntheses, characterization and structures of a mononuclear nickel(II) compound $[Ni^{II}L^1\subset(H_2O)]$ (**1**) and [2 × 1+1 × 2] cocrystals $[\{Ni^{II}L^1M^{II}(H_2O)_3\}\{Ni^{II}L^1\}_2](ClO_4)_2$ [M = Cu (**2**), Ni (**3**), Co (**4**), Fe (**5**) and Mn (**6**)] derived from the hexadentate Schiff base compartmental ligand *N*,*N'*-ethylenebis(3-ethoxysalicylaldimine) (H_2L^1) have been described in this investigation. Compound **1** is an inclusion product in which the water molecule is encapsulated in the O_4 compartment by forming bifurcated hydrogen bonds. Reactions of **1** with perchlorate salts of copper(II), nickel(II), cobalt(II), iron(II) and manganese(II) in open atmosphere produce compounds **2**–**6**, which have similar structures. These compounds are [2 × 1+1 × 2] tetrametallic systems containing self-assembled and cocrystallized one dinuclear $[Ni^{II}L^1M^{II}(H_2O)_3]^{2+}$ cation and two mononuclear $[Ni^{II}L^1]$ moieties. Among three coordinated water molecules of the dinuclear cores in **2**–**6**, two are encapsulated in the O_4 cavity of two mononuclear $[Ni^{II}L^1]$ moieties by forming bifurcated hydrogen bonds. Evidently, the formation of inclusion product **1** and dinuclear–mononuclear cocrystals **2**–**6** are related to the affinity of the O_4 compartment to encapsulate a water molecule. Electrospray ionization mass spectrometry (ESI+) spectra of compounds **1**–**6** have been recorded. The mass spectra of **2**–**6** reveal that not only the tetrametallic self-assemblies are ruptured but also the second metal ion in the dinuclear core leaves the O_4 cavity. For the $Ni^{II}_3Cu^{II}$ (**2**) and $Ni^{II}_3Fe^{II}$ (**5**) compounds, metal substitution takes place in solution, resulting in the formation of $[Cu^{II}L^1Na]^+$ and $[\{Cu^{II}L^1\}_2Na]^+$ for **2** and [1 × 1+1 × 1] species $[\{Ni^{II}L^1\}\cdot\{Fe^{III}L^1\}]^+$ for **5**.

Introduction

Crystal engineering of self-assembled organic and metal–organic systems is an interesting research area.[1,2] Due to extensive development in recent years, it has been possible in many cases to design syntheses of target assemblies, which, in turn, may be useful as functional materials.[1,2]

It is well known that some crystals may contain more than one chemical species and these multicomponent crystals are known as cocrystals.[3–8] It may also be noted that, in comparison to the large number of organic cocrystals,[4–6] multicomponent compounds containing only metal complexes as the components are still rare.[3,7,8] Therefore, we feel that this poorly explored area deserves more attention.

The Schiff base ligands obtained from condensation of 3-ethoxysalicylaldehyde and diamines have been used to derive a number of 3d–4f compounds in which a 3d metal ion occupies the salen-type N_2O_2 cavity and the larger O_4 compartment is occupied by a 4f metal ion.[9] There are a few earlier reports of inclusion of water in the O_4 compartment of a mononuclear system derived from 3-ethoxysalicylaldehyde–diamine Schiff base ligands.[10] We have attempted to explore the possibility of water inclusion in the O_4 compartment of mononuclear copper(II) compounds and observed that the mononuclear copper(II) compounds $[Cu^{II}L^1\subset(H_2O)]$ and $[Cu^{II}L^2\subset(H_2O)]$ derived from *N*,*N'*-ethylenebis(3-ethoxysalicylaldimine) (H_2L^1; Scheme 1) and *N*,*N'*-*o*-phenylenebis(3-ethoxysalicylaldimine) (H_2L^2; Scheme 1) are inclusion products in which the noncoordinated water molecules are encapsulated in the O_4 compartment by forming bifurcated hydrogen bonds.[3a,3b] We have also attempted to explore the nature of copper(II)–3d compounds in these ligand environments and observed that the potential tendency of the O_4 compartment to incorporate a water molecule results in the formation of interesting examples of self-assembled and cocrystallized [2 × 1+1 × 2] and

---

[a] Department of Chemistry, University of Calcutta,
92 A. P. C. Road, Kolkata 700009, India
Fax: +91-33-23519755
E-mail: sm_cu_chem@yahoo.co.in
rk_cu_chem@yahoo.co.in
[b] Institute for Mineralogy and Crystallography, University of Vienna,
Althanstr. 14, 1090 Vienna, Austria
[c] Department of Inorganic Chemistry, Indian Association for the Cultivation of Science,
Kolkata 700032, India
[d] Anorganische and Analytische Chemie, Universität Paderborn,
33098 Paderborn, Germany

Supporting information for this article is available on the WWW under http://dx.doi.org/10.1002/ejic.200900685.

[2 × 2+1 × 3] systems.[3a,3b] We have been interested in exploring whether inclusion phenomena and formation of cocrystals are possible in complexes containing 3d metal ions, other than copper(II), in the salen-type cavity of the related ligands. With this motivation, we report here the syntheses, characterization, crystal structures and mass spectrometry study of the mononuclear nickel(II) compound derived from *N*,*N′*-ethylenebis(3-ethoxysalicylaldimine) (H_2L^1) and the products obtained from the reaction of this mononuclear complex with the perchlorate salts of copper(II), nickel(II), cobalt(II), iron(II) and manganese(II).

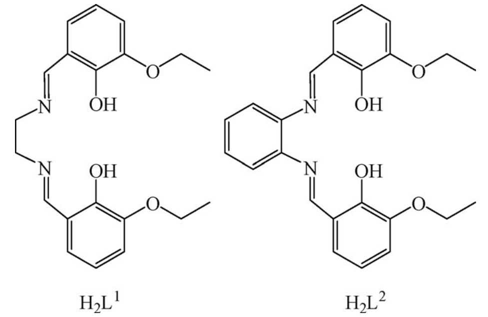

Scheme 1. Chemical structures of the Schiff base ligands H_2L^1 and H_2L^2.

Results and Discussion

Description of the Structure of [$Ni^{II}L^1\subset(H_2O)$] (1)

The crystal structure of [$Ni^{II}L^1\subset(H_2O)$] (**1**) is shown in Figure 1 and selected bond lengths and angles are listed in the caption. The structure of **1** shows that it is a mononuclear compound, and the metal centre is in the salen-type cavity of $[L^1]^{2-}$. One half of the molecule is symmetry related to the other half via a crystallographic twofold axis. The metal–ligand bond lengths involving the imine nitrogen atom [Ni(1)–N(1) 1.8500(15) Å] and the phenoxido oxygen atom [Ni(1)–O(1) 1.8641(12) Å] are almost the same. The N_2O_2 donors form an almost perfect plane, and the metal centre lies exactly on this plane, adopting a square-planar geometry. The *transoid* [178.08(6)°] and *cisoid* [85.82(10)–94.20(6)°] angles in the coordination environment of nickel(II) deviate to a small extent from the ideal values. The water molecule in this compound is hydrogen bonded with the four oxygen atoms and is encapsulated in the acyclic O_4 compartment of $[L^1]^{2-}$. Each of the two water hydrogen atoms forms bifurcated hydrogen bonds with one phenoxido and one ethoxy oxygen atom. The geometries of the hydrogen bonds are summarized in Table 1. The donor···acceptor contacts (2.820 and 3.077 Å) indicate that the hydrogen bonds can be considered as moderately strong; those involving ethoxy oxygen atoms are slightly stronger.

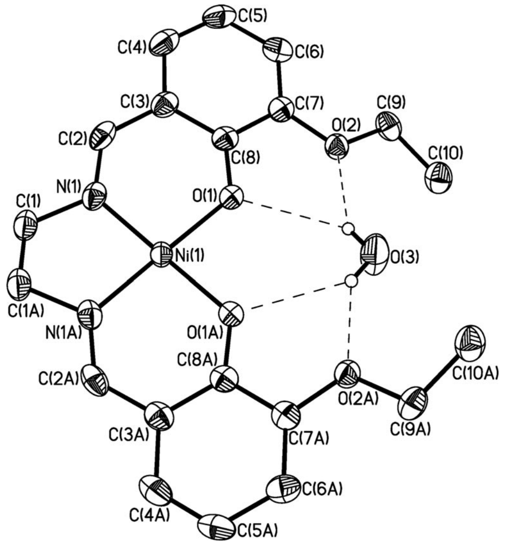

Figure 1. Crystal structure of [$Ni^{II}L^1\subset(H_2O)$] (**1**). Symmetry operations for A: 1 –*x*, *y*, 0.5 – *z*. Selected bond lengths [Å] and angles [°]: Ni(1)–N(1) 1.8500(15), Ni(1)–O(1) 1.8641(12), N(1)–Ni(1)–O(1A) 178.08(6), N(1)–Ni(1)–O(1) 94.20(6), N(1)–Ni(1)–N(1A) 85.82(10), O(1)–Ni(1)–O(1A) 85.84(7).

Table 1. Geometries (distances/Å and angles/°) of the hydrogen bonds responsible for the encapsulation of water in **1**–**6**. Symmetry operations for **2**, B: 1 + *x*, *y*, *z*.

Compound	D–H···A/D···A	D···A	D–H···A
1	O(3)–H(3)···O(1)	3.077	139.3
	O(3)–H(3)···O(2)	2.820	147.7
2	O(3)···O(5B)	2.746	
	O(3)···O(6B)	2.792	
	O(3)···O(7B)	3.006	
	O(3)···O(8B)	2.887	
3	O(3)–H(3A)···O(5)	2.868	
	O(3)–H(3A)···O(7)	2.945	
	O(3)–H(3B)···O(6)	2.800	
	O(3)–H(3B)···O(8)	3.053	
4	O(3)–H(3A)···O(5)	2.882	147.5
	O(3)–H(3A)···O(7)	2.914	140.9
	O(3)–H(3B)···O(6)	2.806	121.8
	O(3)–H(3B)···O(8)	3.003	149.2
5	O(3)–H(3A)···O(5)	2.864	
	O(3)–H(3A)···O(7)	2.898	
	O(3)–H(3B)···O(6)	2.801	
	O(3)–H(3B)···O(8)	3.020	
6	O(3)–H(3A)···O(5)	2.877	144.7
	O(3)–H(3A)···O(7)	2.883	140.1
	O(3)–H(3B)···O(6)	2.812	134.8
	O(3)–H(3B)···O(8)	3.005	151.8

Description of the Structures of [{$Ni^{II}L^1M^{II}(H_2O)_3$}{$Ni^{II}L^1$}$_2$](ClO_4)$_2$ [Cu (2), Ni (3), Co (4), Fe (5) and Mn (6)]

Compounds **2**–**6** crystallize in the same monoclinic *C*2/*c* space group and are isomorphous. As in **1**, one half of the structure of **2**–**6** is symmetry related to the other half by a crystallographic twofold axis. All the structures of **2**–**6** consist of one diphenoxido-bridged dinuclear [$Ni^{II}L^1M^{II}(H_2O)_3$]$^{2+}$ cation, two mononuclear [$Ni^{II}L^1$] moieties and two perchlorate anions. In the dinuclear cores, the N_2O_2

cavity is occupied by a nickel(II) ion, and the second compartment of $[L^1]^{2-}$ is occupied by a second metal centre (Cu^{II}, Ni^{II}, Co^{II}, Fe^{II} and Mn^{II} for **2**, **3**, **4**, **5** and **6**, respectively) that is coordinated to the two bridging phenoxido oxygen atoms and three water molecules. The ethoxy oxygen atoms of the ligand remain noncoordinated. As discussed below, the diphenoxido-bridged $[Ni^{II}L^1M^{II}(H_2O)_3]^{2+}$ cation is self-assembled with two mononuclear $[Ni^{II}L^1]$ species by hydrogen-bonding interactions. The crystal structures of **2** and **6** are shown in Figures 2 and 3, respectively, whereas the structures of **3**–**5** are represented in Figures S1–S3 (Supporting Information).

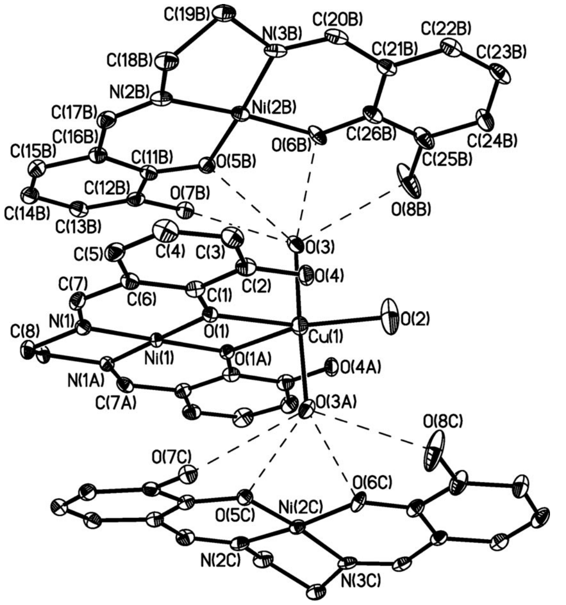

Figure 2. Structure of the $Ni^{II}_3Cu^{II}$ compound **2** showing [2 × 1+1 × 2] self-assembly of the dinuclear $[Ni^{II}L^1Cu^{II}(H_2O)_3]^{2+}$ cation and two mononuclear $[Ni^{II}L^1]$ moieties. Hydrogen atoms and the perchlorate anions are omitted for clarity. Carbon atoms of the ethoxy moieties have been omitted for better representation of the hydrogen bonds. Symmetry operations for A: 2 –*x*, *y*, 0.5 – *z*; B: 1 + *x*, *y*, *z*; C: 1 – *x*, *y*, 0.5 – *z*.

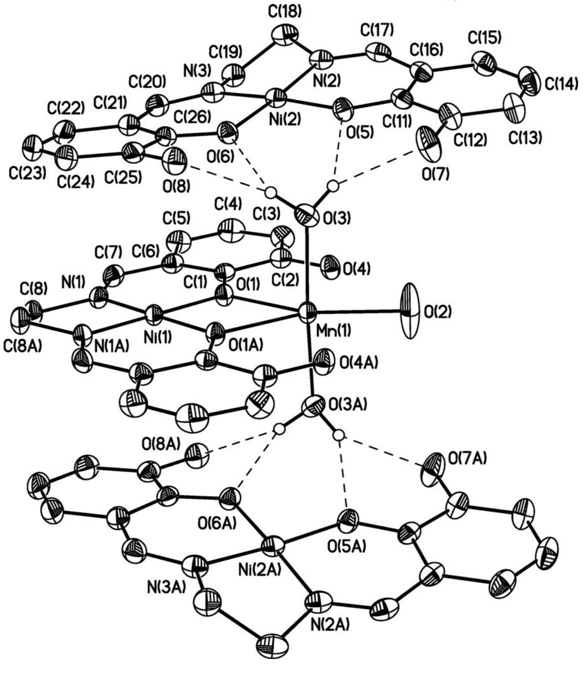

Figure 3. Structure of the $Ni^{II}_3Mn^{II}$ compound **6** showing [2 × 1+1 × 2] self-assembly of the dinuclear $[Ni^{II}L^1Mn^{II}(H_2O)_3]^{2+}$ cation and two mononuclear $[Ni^{II}L^1]$ moieties. Hydrogen atoms, except those of encapsulated water molecules, and the perchlorate anions are omitted for clarity. Carbon atoms of the ethoxy moieties have been omitted for better representation of the hydrogen bonds. Symmetry operations for A: –*x*, *y*, 0.5 – *z*.

The metrical parameters of the coordination environment of two crystallographically different nickel(II) centres in the salen-type cavity in **2**–**6** are summarized in Table S1 (Supporting Information). The square planar environments in these cases are similar to that in compound **1**.

The second metal centre in the dinuclear core in **2**–**6** is pentacoordinated by two phenoxido oxygen atoms [O(1) and O(1A)] and three water oxygen atoms [O(2), O(3) and O(3A)]. The bond lengths and angles of the MO_5 coordination environment in **2**–**6** are summarized in Table 2. The metal–O(water) bond lengths in these compounds are either equal [2.141(4) and 2.144(2) Å in **6**] or differ only slightly [2.076(3) and 2.080(5) Å in **5**; 2.086(5) and 2.098(6) Å in **4**; 1.946(14) and 1.953(6) Å in **3**; 1.935(4) and 1.987(8) Å in **2**]. In comparison, the metal–O(phenoxido) bond lengths [2.186(4), 2.147(4), 2.176(3), 2.164(2) and 2.198(2) Å, respectively for **2**, **3**, **4**, **5** and **6**] are longer. Regarding metal–water bond lengths in the present series, the order is $Mn^{II} > Co^{II} \approx Fe^{II} > Cu^{II} \approx Ni^{II}$. It may be relevant to compare the metal–water bond lengths in **2**–**6** with those of reported related compounds derived from similar ligands. The Mn^{II}–water bond lengths (2.15–2.21 Å) in two $Cu^{II}_3Mn^{II}$ compounds are much longer than the Cu^{II}–water bond lengths (1.91–1.97 Å) in Cu^{II}_4 and Cu^{II}_7 compounds, whereas Co^{II}–water bond length (2.04 Å) in a $Cu^{II}_3Co^{II}$ compound is in between the Mn^{II}–water and Cu^{II}–water bond lengths.[3a,3b] Clearly, the M^{II}–water bond length for a particular metal ion in the title compounds and in the reported examples are very close. There are many compounds containing coordinated water molecules,[11] in which the metal–water bond lengths are definitely dependent on the other ligands and therefore a correlation should not be obtained. However, although $[M(H_2O)_6]^{2+}$ systems may also be influenced by crystal packing effects of the environment, these are better systems to make a comparison of the relative magnitude of metal–water bond lengths. In most cases, the usual ranges are as follows: Cu^{II}–water (equatorial) < 2 Å, Cu^{II}–water (axial) > 2.3 Å, Ni^{II}–water ≈ 2.0–2.05 Å, Co^{II}–water ≈ 2.05–2.15 Å, Fe^{II}–water ≈ 2.05–2.15 Å and Mn^{II}–water ≈ 2.14–2.27 Å.[11] The order can be considered as similar to that observed in the title compounds. Again, it can be clear from the two cases {title and related compounds; $[M(H_2O)_6]^{2+}$} that the Mn^{II}–water bond length should be much longer than either of the Ni^{II}–water and Cu^{II}–water (equatorial for hexacoordination) bond lengths.

Table 2. Selected bond lengths/Å and angles/° in the coordination environment of the pentacoordinate metal centres in the dinuclear cores of **2**–**6**. Symmetry operations for **2**, A: 2 –*x*, *y*, 0.5 – *z*. Symmetry operations for **3**–**6**, A: –*x*, *y*, 0.5 – *z*.

2			
Cu(1)–O(1)	2.186(4)	Cu(1)–O(3)	1.935(4)
Cu(1)–O(2)	1.987(8)		
O(3)–Cu(1)–O(3A)	178.2(3)	O(1)–Cu(1)–O(3A)	91.14(17)
O(1)–Cu(1)–O(2)	145.24(10)	O(2)–Cu(1)–O(3)	89.08(13)
O(1)–Cu(1)–O(1A)	69.5(2)	Ni(1)–O(1)–Cu(1)	103.51(17)
O(1)–Cu(1)–O(3)	90.37(17)		
3			
Ni(3)–O(1)	2.147(4)	Ni(3)–O(3)	1.953(6)
Ni(3)–O(2)	1.946(14)		
O(3)–Ni(3)–O(3A)	175.9(3)	O(1)–Ni(3)–O(3A)	91.45(19)
O(1)–Ni(3)–O(2)	145.28(11)	O(2)–Ni(3)–O(3)	87.97(15)
O(1)–Ni(3)–O(1A)	69.4(2)	Ni(1)–O(1)–Ni(3)	103.94(18)
O(1)–Ni(3)–O(3)	91.88(18)		
4			
Co(1)–O(1)	2.176(3)	Co(1)–O(3)	2.086(5)
Co(1)–O(2)	2.098(6)		
O(3)–Co(1)–O(3A)	177.5(3)	O(1)–Co(1)–O(3A)	89.85(17)
O(1)–Co(1)–O(2)	146.00(7)	O(2)–Co(1)–O(3)	88.74(14)
O(1)–Co(1)–O(1A)	68.00(14)	Ni(1)–O(1)–Co(1)	104.85(12)
O(1)–Co(1)–O(3)	92.24(14)		
5			
Fe(1)–O(1)	2.1636(18)	Fe(1)–O(3)	2.076(3)
Fe(1)–O(2)	2.080(5)		
O(3)–Fe(1)–O(3A)	176.93(14)	O(1)–Fe(1)–O(3A)	90.16(9)
O(1)–Fe(1)–O(2)	145.85(5)	O(2)–Fe(1)–O(3)	88.46(7)
O(1)–Fe(1)–O(1A)	68.29(10)	Ni(1)–O(1)–Fe(1)	104.71(8)
O(1)–Fe(1)–O(3)	92.39(8)		
6			
Mn(1)–O(1)	2.1981(16)	Mn(1)–O(3)	2.144(2)
Mn(1)–O(2)	2.141(4)		
O(3)–Mn(1)–O(3A)	176.99(13)	O(1)–Mn(1)–O(3A)	89.98(8)
O(1)–Mn(1)–O(2)	146.67(4)	O(2)–Mn(1)–O(3)	88.50(6)
O(1)–Mn(1)–O(1A)	66.67(8)	Ni(1)–O(1)–Mn(1)	105.65(7)
O(1)–Mn(1)–O(3)	92.54(8)		

The MO_5 coordination environment (Figures 2 and 3, Table 2; Figures S1–S3, Supporting Information) in **2**–**6** is highly distorted. The values of τ in this coordination environment are 0.55, 0.51, 0.52, 0.52 and 0.51 for **2**, **3**, **4**, **5** and **6**, respectively, indicating that the geometry of the second metal centre in the dinuclear core is intermediate between square pyramidal and trigonal bipyramidal.[3a] In the case of a square pyramidal environment, one phenoxido oxygen atom [either of O(1) or O(1A)] can be considered as the apical atom; the remaining phenoxido oxygen atom [O(1) or O(1A)] and the three water oxygen atoms [O(2), O(3) and O(3A)] occupy the equatorial positions. The average deviations of the four basal oxygen atoms from the least-squares O_4 plane is ca. 0.30 Å, and the pentacoordinate metal centre is displaced by ca. 0.30 Å from this plane. For trigonal bipyramidal geometry, two phenoxido oxygen atoms [O(1) and O(1A)] and one water oxygen atom [O(2)] define the equatorial plane; the two remaining water oxygen atoms [O(3) and O(3A)] occupy the apical positions. There should be three sets of bond angles for perfect trigonal bipyramidal geometry: one of 180°, six of 90° and three of 60°. Again, for perfect square pyramidal environment, there should be two angles of 180° and eight of 90°. For **2**–**6**, one angle is close to 180° [178.2(3), 175.9(3), 177.5(3), 176.9(1) and 177.0(1)° for **2**, **3**, **4**, **5** and **6**, respectively], whereas the range of other angles is much wider [69.5(2)–145.24(10)° for **2**; 69.4(2)–145.3(1)° for **3**; 68.0(1)–146.0(1)° for **4**; 68.3(1)–145.8(1)° for **5**; 66.7(1)–146.7(1)° for **6**]. Clearly, the geometry of the second metal centre in the dinuclear cores in **2**–**6** is far from both perfect square pyramidal and trigonal bipyramidal and therefore should be considered as an intermediate of the two.

If two ethoxy oxygen atoms [O(4) and O(4A)] are also considered as part of the coordination sphere, the coordination environment of the second metal centre would be heptacoordinated pentagonal bipyramidal; the five oxygen atoms [O(1), O(1A), O(2), O(4) and O(4A)] define the pentagonal plane and the remaining oxygen atoms [O(3) and O(3A)] occupy the axial positions. The constituent atoms are deviated only a little (<0.04 Å) from the least-squares O_5 plane and the metal ion is pocketed in this plane. Again, the trans angle [O(3)–M–O(3A) 175.9(3)–178.2(3)°] is very close to 180°, indicating apparently a small extent of distortion of the pentagonal bipyramidal geometry. However, the wide range of bond lengths in the pentagonal plane (1.93–2.65 Å for **2**; 1.95–2.59 Å for **3**; 2.08–2.54 Å for **4**; 2.08–2.53 Å for **5**; 2.14–2.52 Å for **6**), indicate appreciable distortion of the heptacoordinated coordination environment. Clearly, the source of these distortions is the long M–O(ethoxy) bond lengths. Interestingly, the M–O(ethoxy) bond lengths in **2**–**6** follow the consistent order $\mathrm{Mn^{II}}$ (2.52 Å) < $\mathrm{Fe^{II}}$ (2.53 Å) < $\mathrm{Co^{II}}$ (2.54 Å) < $\mathrm{Ni^{II}}$ (2.59 Å) < $\mathrm{Cu^{II}}$ (2.65 Å). Anyway, it is difficult to conclude the coordination number and coordination geometry of the second metal centres in **2**–**6**. It may be five coordinated MO_5, in which the geometry is intermediate between distorted square pyramidal and distorted trigonal bipyramidal, or seven coordinated MO_7, in which the geometry is distorted pentagonal bipyramidal. However, it may be better to discard the heptacoordinated environment on the basis of the longer M–O(ethoxy) bond lengths (>2.5 Å).[3b]

The Ni(1)–O(1)–M bridge angles in the dinuclear cores are very close and considering all the five complexes, the range of these angles is very small [103.51(17)–105.65(7)°; Table 2]. The metal···metal separation varies in the small range of 3.15–3.22 Å. The bridging moiety in the dinuclear core is highly twisted, as evidenced by the dihedral angles (90.9, 91.0, 92.7, 92.5 and 92.9° for **2**, **3**, **4**, **5** and **6**, respectively) between the N_2O_2 square plane of the nickel(II) centre and the equatorial O_4 basal plane (for the distorted square pyramidal geometry) of the second metal environment.

As in **1**, water encapsulation due to the formation of bifurcated hydrogen bonds in the O_4 compartment takes place also in compounds **2**–**6**. The O_4 cavities of the two $[\mathrm{Ni^{II}L^1}]$ moieties are occupied by two coordinated water molecules (Figures 2 and 3; Figure S1–S3, Supporting Information). The geometries of the hydrogen bonds are summarized in

Table 1. The O···O contacts are in the range 2.75–3.05 Å, and the hydrogen bonds may be considered as moderately strong.

Synthesis and Characterization

Reaction of nickel(II) acetate tetrahydrate and H_2L^1 produces the mononuclear nickel(II) complex $[Ni^{II}L^1\subset(H_2O)]$ (**1**). As already discussed, the water molecule in **1** is hydrogen bonded to the phenolate oxygen atoms and also to the oxygen atoms of the ethoxy side chains, resulting in the formation of an inclusion product. When **1** is treated with $M(ClO_4)_2{\cdot}6H_2O$, the compounds $[\{Ni^{II}L^1M^{II}(H_2O)_3\}\{Ni^{II}L^1\}_2](ClO_4)_2$ [M = Cu (**2**), Ni (**3**), Co (**4**), Fe (**5**) and Mn (**6**)] separate from the solution as red or orange crystals. Compared to the $\nu_{C=N}$ vibration observed in the free H_2L^1 ligand at 1627 cm^{-1}, this vibration is shifted slightly and appears in the range 1621–1630 cm^{-1} in complexes **2**–**6**. The IR spectrum of **1** exhibits two weak but sharp signals at 3578 and 3528 cm^{-1} (Figure 4), which is due to the asymmetric and symmetric stretching of the encapsulated water molecule.[3a,3b] The motion of water due to encapsulation is so restricted that the bending vibration is also observed for **1** as a weak intensity band at 1547 cm^{-1}.[3a,3b] As compounds **2**–**6** contain both the encapsulated and non-encapsulated water molecules and the extent of encapsulation is less (vide infra), the water stretching modes appear as a broad band in the range 3382–3425 cm^{-1}. The characteristic perchlorate signals are observed for compounds **2**–**6** as a very strong band at ca. 1090 cm^{-1} and as a weak band at ca. 621 cm^{-1}.

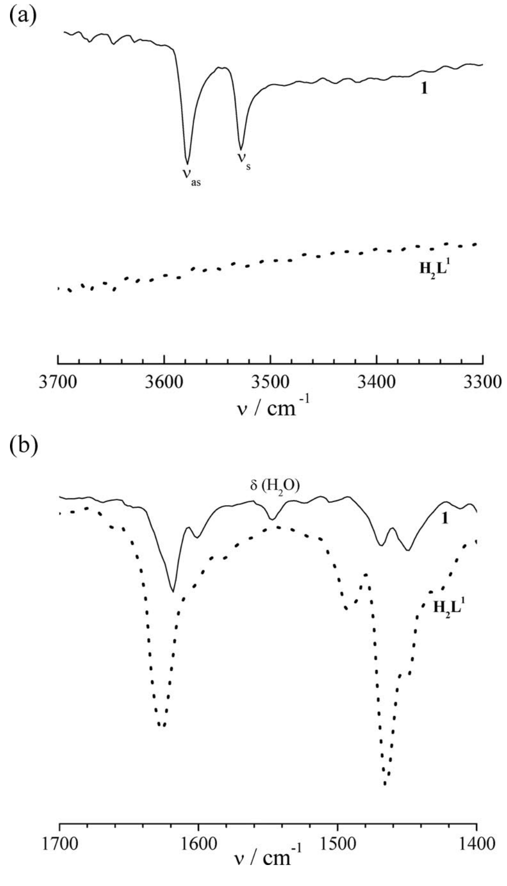

Figure 4. Part of the IR spectrum of H_2L^1 and $[Ni^{II}L^1\subset(H_2O)]$ (**1**) demonstrating (a) stretching and (b) bending vibrations of the encapsulated water molecule in **1**.

As usual for square planar nickel(II) systems, compound **1** is diamagnetic. The room-temperature magnetic moment values of the $Ni^{II}_3Cu^{II}$ (**2**), Ni^{II}_4 (**3**), $Ni^{II}_3Co^{II}$ (**4**), $Ni^{II}_3Fe^{II}$ (**5**) and $Ni^{II}_3Mn^{II}$ (**6**) compounds are, respectively, 1.82, 2.78, 4.62, 5.01 and 5.84 BM, which indicates that the paramagnetic moment arises only due to the second metal centre in the dinuclear core. In comparison to the spin only value of 3.87 BM for high-spin cobalt(II), the larger observed moment of compound **4** is related to the usual first-order orbital angular momentum of this metal ion. The room-temperature magnetic moment values of **2**–**6** indicate that, as in **1**, the three square planar nickel(II) centres in **2**–**6** are diamagnetic and therefore superexchange is not possible in these compounds.

Electrospray Ionization Mass Spectral Study of 1–6

The electrospray ionization mass spectra (ESI+) of compounds **1**–**6** were recorded in acetonitrile solutions. The spectrum of $[Ni^{II}L^1\subset(H_2O)]$ (**1**; Figure 5) exhibits three peaks at *m*/*z* (%) = 413 (4), 434.86 (100) and 846.80 (60), which are assignable to the monocationic species $[Ni^{II}L^1H]^+$ ($C_{20}H_{23}N_2O_4Ni$), $[Ni^{II}L^1Na]^+$ ($C_{20}H_{22}N_2O_4NiNa$) and $[\{Ni^{II}L^1\}_2Na]^+$ ($C_{40}H_{44}N_4O_8Ni_2Na$), respectively. As shown in Figure 5, the isotopic distribution patterns of the observed peaks and the simulated spectral patterns are in excellent agreement with each other. The site of protonation for $[Ni^{II}L^1H]^+$ is not clear. However, it is evident that the sodium(I) ion in $[Ni^{II}L^1Na]^+$ occupies the O_4 cavity of the ligand, forming a diphenoxido-bridged $Ni^{II}Na^I$ species. Again, in $[\{Ni^{II}L^1\}_2Na]^+$, the sodium(I) ion is probably coordinated to two O_4 cavities and is thus sandwiched in between two mononuclear $[Ni^{II}L^1]$ species.

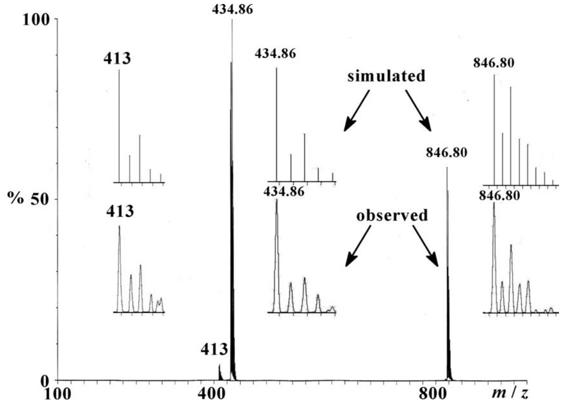

Figure 5. Mass spectrum (ESI+) of $[Ni^{II}L^1\subset(H_2O)]$ (**1**) in acetonitrile showing observed and simulated isotopic distribution pattern.

As observed for the mononuclear compound [$Ni^{II}L^1{\subset}(H_2O)$] (**1**), signals of [$Ni^{II}L^1H$]$^+$, [$Ni^{II}L^1Na$]$^+$ and [$\{Ni^{II}L^1\}_2Na$]$^+$ are observed in the mass spectra (Figure 6; Figure S4, Supporting Information) of the $Ni^{II}_3Mn^{II}$ and $Ni^{II}_3Co^{II}$ compounds [$\{Ni^{II}L^1M^{II}(H_2O)_3\}\{Ni^{II}L^1\}_2$]($ClO_4$)$_2$ [M = Mn (**6**) and Co(**4**)]. For the Ni^{II}_4 compound [$\{Ni^{II}L^1Ni^{II}(H_2O)_3\}\{Ni^{II}L^1\}_2$]($ClO_4$)$_2$ (**3**), two peaks at *m*/*z* (%) = 434.94 (100) and 846.91 (8) (Figure S5, Supporting Information) arise due to [$Ni^{II}L^1Na$]$^+$ and [$\{Ni^{II}L^1\}_2Na$]$^+$, respectively; in this case, the protonated species [$Ni^{II}L^1H$]$^+$ is not formed. The molecular weights for the tetra- or dimetallic dications [$\{Ni^{II}L^1M^{II}(H_2O)_3\}\{Ni^{II}L^1\}_2$]$^{2+}$, [$\{Ni^{II}L^1M^{II}\}\{Ni^{II}L^1\}_2$]$^{2+}$, [$Ni^{II}L^1M^{II}(H_2O)_3$]$^{2+}$ and [$Ni^{II}L^1M^{II}$]$^{2+}$ (M = Ni, Co and Mn for **3**, **4** and **6**, respectively) vary between 1348.29–1352.28, 1294.24–1298.23, 522.08–526.08 and 468.04–472.04, respectively. As no peaks in these ranges are observed in the mass spectra, it is evident not only that the hydrogen bonded self-assembly is ruptured in solution but also that the second metal centre (Ni, Co or Mn) leaves the O_4 cavity. Therefore, it is clear that incorporation of a second 3d metal centre is governed by the formation of self-assembly; as the self-assembly is broken in solution, the dinuclear 3d–3d core becomes nonexistent. The instability of the tetrametallic or dimetallic cores is also evident from the fact that the solution of the [2 × 1+1 × 2] self-assemblies **2**–**6** produce the mononuclear inclusion product [$Ni^{II}L^1{\subset}(H_2O)$] (**1**) (vide infra).

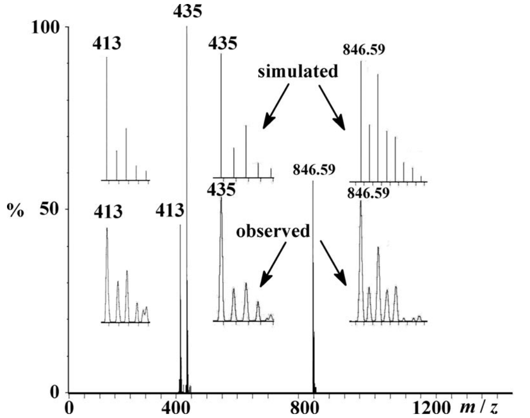

Figure 6. Mass spectrum (ESI+) of [$\{Ni^{II}L^1Mn^{II}(H_2O)_3\}\{Ni^{II}L^1\}_2$]($ClO_4$)$_2$ (**6**) in acetonitrile showing observed and simulated isotopic distribution pattern.

The spectrum of the $Ni^{II}_3Cu^{II}$ compound [$\{Ni^{II}L^1Cu^{II}(H_2O)_3\}\{Ni^{II}L^1\}_2$]($ClO_4$)$_2$ (**2**; Figure 7) exhibits four peaks at *m*/*z* (%) = 434.96 (48), 846.95 (5), 439.96 (100) and 856.92 (32). Whereas the first two peaks arise due to [$Ni^{II}L^1Na$]$^+$ and [$\{Ni^{II}L^1\}_2Na$]$^+$, respectively, the third and fourth are well matched with the species [$Cu^{II}L^1Na$]$^+$ and [$\{Cu^{II}L^1\}_2Na$]$^+$, respectively. Clearly, copper(II) leaves the O_4 cavity in solution and substitutes Ni^{II} from the N_2O_2 compartment to form [$Cu^{II}L^1$] species, which in turn, produces dinuclear $Cu^{II}Na^I$ and trinuclear $Cu^{II}Na^ICu^{II}$ species during recording of the mass spectrum. The greater intensities of the $Cu^{II}Na^ICu^{II}$ (32%) and $Cu^{II}Na^I$ (100%) peaks in comparison to those of the nickel(II) analogues $Ni^{II}Na^INi^{II}$ (5%) and $Ni^{II}Na^I$ (48%) indicate that the copper(II) species are more stable on the timescale of the mass spectrometer.

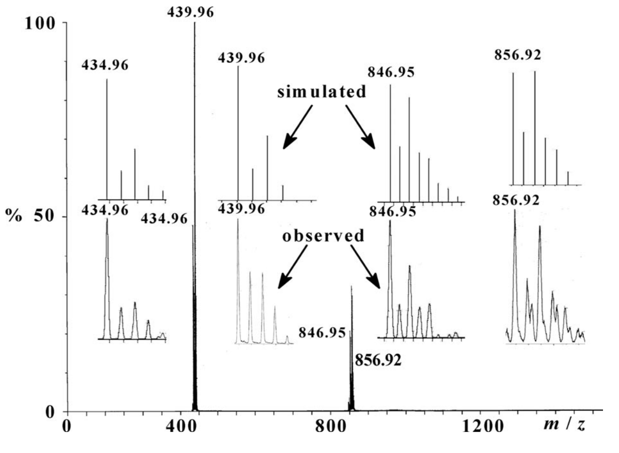

Figure 7. Mass spectrum (ESI+) of [$\{Ni^{II}L^1Cu^{II}(H_2O)_3\}\{Ni^{II}L^1\}_2$]($ClO_4$)$_2$ (**2**) in acetonitrile showing observed and simulated isotopic distribution pattern.

Three peaks at *m*/*z* (%) = 413 (28), 434.9 (100) and 822 (5) are observed in the spectrum of the $Ni^{II}_3Fe^{II}$ compound [$\{Ni^{II}L^1Fe^{II}(H_2O)_3\}\{Ni^{II}L^1\}_2$]($ClO_4$)$_2$ (**5**; Figure 8). Whereas the 413 and 434.9 peaks are assignable to [$Ni^{II}L^1H$]$^+$ and [$Ni^{II}L^1Na$]$^+$, respectively, the low-intensity peak at *m*/*z* = 822 can be assignable to a [1 × 1+1 × 1] species [$Ni^{II}L^1$]·[$Fe^{III}L^1$] ($C_{40}H_{44}N_4O_8NiFe$). As shown in Figure 8, the isotopic distribution is well matched with the observed spectrum, indicating the correct assignment. Clearly, Fe^{II} that leaves the O_4 cavity substitutes Ni^{II} from the N_2O_2 cavity and becomes oxidized to form a Fe^{III}–salen-type compound. The semicoordination of the phenoxido oxygen atoms of the [$Ni^{II}L^1$] moiety to Fe^{III} of the [$Fe^{III}L^1$]$^+$ moiety is probably the reason for the formation of the [1 × 1+1 × 1] self-assembly (Figure 9) during the recording of the mass spectrum.

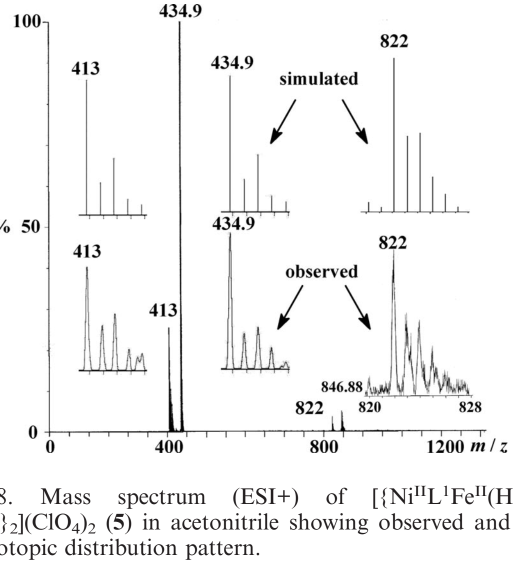

Figure 8. Mass spectrum (ESI+) of [$\{Ni^{II}L^1Fe^{II}(H_2O)_3\}\{Ni^{II}L^1\}_2$]($ClO_4$)$_2$ (**5**) in acetonitrile showing observed and simulated isotopic distribution pattern.

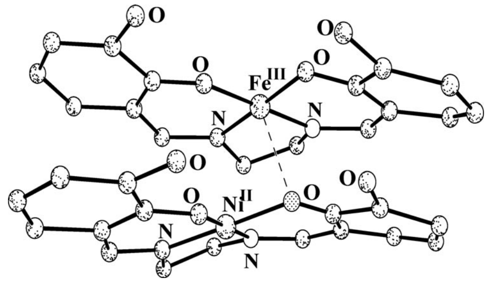

Figure 9. [1 × 1+1 × 1] cocrystal $[Ni^{II}L^1]\cdot[Fe^{III}L^1]^+$.

Comparison of the Compositions of 1–6 with the Related Compounds Containing Copper(II) in the Salen-Type Cavity of *N*,*N′*-Ethylenebis(3-ethoxysalicylaldimine) (H_2L^1)

The mononuclear compounds $[Ni^{II}L^1\subset(H_2O)]$ (**1**) and $[Cu^{II}L^1\subset(H_2O)]$ (**7**)[3a] are both inclusion products. Treatment of the perchlorate salts of copper(II), cobalt(II) and manganese(II) with **7** under an open atmosphere results in the self-assembled [2 × 1+1 × 2] cocrystals $[\{Cu^{II}L^1M^{II}(H_2O)_3\}\{Cu^{II}L^1\}_2](ClO_4)_2$ [M^{II} = Cu (**8**), Co (**9**), Mn (**10**)] containing self-assembled and cocrystallized single dinuclear $[Cu^{II}L^1M^{II}(H_2O)_3]^{2+}$ cationic and two mononuclear $[Cu^{II}L^1]$ units.[3a] Treatment of $[Cu^{II}L^1\subset(H_2O)]$ (**7**) with nickel(II) perchlorate produces a system having the apparent composition $[Cu^{II}L^1Ni^{II}(H_2O)_3](ClO_4)_2\cdot3[Cu^{II}L^1]$ (**11**).[3a] Again, the reaction of iron(II) perchlorate with **7** under an open atmosphere produces a mononuclear–mononuclear [1 × 1+1 × 1] cocrystal $[Cu^{II}L^1\subset(H_2O)]\cdot[\{Fe^{III}L^1(H_2O)_2\}(ClO_4)]$ (**12**).[12] Evidently, although the products obtained from the reaction of the copper(II) inclusion compound $[Cu^{II}L^1\subset(H_2O)]$ (**7**) with the perchlorate salts of copper(II), cobalt(II) and manganese(II) are similar tetranuclear cocrystals, the compositions of the products obtained from the reaction of **7** with the perchlorate salts of iron(II) and nickel(II) are different. In contrast, the reactions of the nickel(II) mononuclear compound $[Ni^{II}L^1\subset(H_2O)]$ (**1**) with the perchlorate salts of copper(II), nickel(II), cobalt(II), iron(II) and manganese(II) under an open atmosphere produce similar [2 × 1+1 × 2] cocrystals $[\{Ni^{II}L^1M^{II}(H_2O)_3\}\{Ni^{II}L^1\}_2](ClO_4)_2$ (**2**–**6**) containing self-assembled dinuclear and mononuclear moieties.

The relative extent of the encapsulation of water may be understood from the displacement (d_O) of the water oxygen atom from the least-squares $O(phenoxido)_2O(ethoxy)_2$ plane. In the case of $[Ni^{II}L^1\subset(H_2O)]$ (**1**) and previously reported compound $[Cu^{II}L^1\subset(H_2O)]$ (**7**), the oxygen atom of the encapsulated water lies on the least-squares $O(phenoxido)_2O(ethoxy)_2$ plane, whereas the oxygen atoms of the encapsulated water molecules in $[\{Ni^{II}L^1M^{II}(H_2O)_3\}\{Ni^{II}L^1\}_2](ClO_4)_2$ (**2**–**6**) and in $[\{Cu^{II}L^1M^{II}(H_2O)_3\}\{Cu^{II}L^1\}_2](ClO_4)_2$ (**8**–**10**) are displaced by 1.28–1.53 and 0.92–1.23 Å, respectively, from the corresponding $O(phenoxido)_2O(ethoxy)_2$ plane, indicating that the extent of encapsulation in the mononuclear inclusion products **1** and **7** is much greater than that in the cocrystalline compounds **2**–**6** or **8**–**10**. It is also evident that the extent of encapsulation in the previous series **8**–**10** is slightly better than that in the present series **2**–**6**.

It should be noted that treatment of compounds **2**–**6** and **8**–**10** with dimethylformamide results in the formation of compound **1** and **7**, respectively, indicating that the O_4 compartment is preferable for water in both systems. Again, in both systems, the formation of a 3d–4f or 3d–3d bimetallic core from the mononuclear inclusion product and the decomposition of the former to the latter by dimethylformamide resemble the transmetallation reaction. This behaviour can be considered as the resemblance of water with metal ions.

Conclusions

The present study is concerned with the designed syntheses of an inclusion compound and dinuclear–mononuclear cocrystals in the systems containing 3d metal ions, other than copper(II), in the salen-type compartment of 3-ethoxysalicylaldehyde–diamine Schiff base ligands. The formation of the mononuclear nickel(II) inclusion product (**1**) and the dinuclear–mononuclear cocrystals (**2**–**6**) derived from *N*,*N′*-ethylenebis(3-ethoxysalicylaldimine) (H_2L^1) have been the major outcome of the present investigation. It has been evident from this and previous studies that inclusion products and dinuclear–mononuclear cocrystals are stabilized in the complexes containing either nickel(II) or copper(II)[3a] in the salen-type compartment. In both series, the reason for the formation of inclusion products and dinuclear–mononuclear cocrystals is the tendency of the O_4 compartment of the Schiff base ligand to encapsulate a water molecule. It may also be noted that, in contrast to the difference in composition of the products (**8**–**10**) obtained from the reaction of mononuclear copper(II) compounds with perchlorate salts of 3d metal ions, the 3d–3d systems (**2**–**6**) are self-assembled compounds containing one dinuclear and two mononuclear moieties. Evidently, it can be concluded that, between $[Ni^{II}L^1\subset(H_2O)]$ (**1**) and $[Cu^{II}L^1\subset(H_2O)]$ (**7**), the former is more potential to derive [2 × 1+1 × 2] systems and cocrystals. It also seems that square-planar geometry of the metal ion in the salen-type cavity of the mononuclear compounds {as in $[Ni^{II}L^1\subset(H_2O)]$ (**1**) and $[Cu^{II}L^1\subset(H_2O)]$ (**7**)} is a condition to produce dinuclear–mononuclear cocrystals. However, the combination of metal ions is another factor definitely; whereas $Cu^{II}_3Ni^{II}$ and $Cu^{II}_3Fe^{II}$ are not possible, $Ni^{II}_3Ni^{II}$ and $Ni^{II}_3Fe^{II}$ complexes can be isolated. The ESI-MS (positive) study presented in this investigation is an interesting aspect. The spectra clearly indicate that tetrametallic self-assembly and also the $Ni^{II}M^{II}$ dinuclear core is unstable in solution. It is also evident from this mass spectroscopic study that incorporation of the second metal ion in the O_4 cavity is governed by the formation of tetrametallic self-assembly. Again, formation of positive ions containing copper(II) or iron(III) in the N_2O_2 cavity during the recording of the mass spectra indicates metal substitution reactions. Interestingly, the formation of a new [1 × 1+1 × 1] self-assembly, $[Ni^{II}L^1]\cdot[Fe^{III}L^1]$, has been evidenced from the mass spectra of **5**. The area of inclusion phenomena and cocrystallization in the related ligand systems using various metal combinations may result in interesting results and those works are under progress in our laboratory.

Experimental Section

Materials and Physical Methods: All reagents and solvents were purchased from commercial sources and used as received. The Schiff base ligand H_2L^1 was prepared by 2:1 condensation of 3-ethoxysalicylaldehyde and ethylenediamine in methanol.[3a,9a] Elemental (C, H, and N) analyses were performed with a Perkin–Elmer 2400 II analyzer. IR spectra were recorded in the region 400–4000 $\mathrm{cm^{-1}}$ with a Perkin–Elmer RXIFT spectrophotometer with samples as KBr disks. Magnetic susceptibility measurements of **1**–**6** at 300 K were carried out with a Sherwood Scientific Co., UK magnetic susceptibility balance. The electrospray ionization mass spectra of **1**–**6** were recorded with a Micromass Qtof YA 263 mass spectrometer.

$[\mathrm{Ni^{II}L^1}\subset(\mathrm{H_2O})]$ (1):[9a] An aqueous solution (20 mL) of nickel(II) acetate tetrahydrate (1.25 g, 5 mmol) was added dropwise to a suspension of H_2L^1 (1.78 g, 5 mmol) in methanol (40 mL). A reddish precipitate started to deposit. After stirring for a few hours, the compound was collected by filtration and air dried. Recrystallization from dimethylformamide yielded a dark red crystalline compound containing crystals suitable for X-ray diffraction. Yield: 1.83 g (85%). Diamagnetic. $C_{20}H_{24}N_2NiO_5$ (431.13): calcd. C 55.72, H 5.61, N 6.50; found C 55.64, H 5.68, N 6.55. IR (KBr): $\tilde{\nu}$ = 3578 (w) [$\nu_{as}(H_2O)$], 3528 (w) [$\nu_s(H_2O)$], 1618 (s) [ν(C=N)], 1547 (w) [$\delta(H_2O)$] $\mathrm{cm^{-1}}$.

$[\{\mathrm{Ni^{II}L^1M^{II}(H_2O)_3}\}\{\mathrm{Ni^{II}L^1}\}_2](\mathrm{ClO_4})_2$ [M = Cu (2), Ni (3), Co (4), Fe (5), and Mn (6)]: These five compounds were prepared in the same way as that described below for **3** by using the appropriate $M(ClO_4)_2 \cdot 6H_2O$. All these compounds were synthesized under an open atmosphere, that is, no caution was required to prevent possible oxidation/oxygenation phenomena with systems containing even $\mathrm{Co^{II}}$ or $\mathrm{Fe^{II}}$.

A solution of **1** (0.108 g, 0.25 mmol) in dichloromethane/methanol (3:1, 15 mL) was added dropwise with stirring to a methanol solution (5 mL) of nickel(II) perchlorate hexahydrate (0.091 g, 0.25 mmol). After 1 h stirring, the red solution was filtered to remove any suspended particles. The filtrate was then kept at room temperature for slow evaporation. After a few hours, dark red crystals of **3** suitable for X-ray diffraction deposited and were collected and washed with acetone. Yield: 0.11 g (85%). $C_{60}H_{72}Cl_2N_6Ni_4O_{23}$ (1551.00): calcd. C 46.47, H 4.68, N 5.42; found C 46.56, H 4.60, N 5.48. IR (KBr): $\tilde{\nu}$ = 3414 (w) [νO–H(water)]; 1622 (s) [ν(C=N)]; 1088 (vs), 620 (w) [$\nu(ClO_4)$]$\mathrm{cm^{-1}}$. μ_{eff} = 2.78 BM.

2: Red crystals. Yield: 80%. $C_{60}H_{72}Cl_2CuN_6Ni_3O_{23}$ (1555.84): calcd. C 46.32, H 4.66, N 5.40; found C 46.38, H 4.60, N 5.45. IR (KBr): $\tilde{\nu}$ = 3382 (w) [νO–H(water)]; 1630 (s) [ν(C=N)]; 1089 (vs), 621 (w) [$\nu(ClO_4)$] $\mathrm{cm^{-1}}$. μ_{eff} = 1.82 BM.

4: Orange crystals. Yield: 80%. $C_{60}H_{72}Cl_2CoN_6Ni_3O_{23}$ (1551.22): calcd. C 46.46, H 4.68, N 5.42; found C 46.54, H 4.74, N 5.49. IR (KBr): $\tilde{\nu}$ = 3412 (w) [νO–H(water)]; 1621 (s) [ν(C=N)]; 1090 (vs), 622 (w) [$\nu(ClO_4)$] $\mathrm{cm^{-1}}$. μ_{eff} = 4.62 BM.

5: Red crystals. Yield: 82%. $C_{60}H_{72}Cl_2FeN_6Ni_3O_{23}$ (1548.14): calcd. C 46.55, H 4.69, N 5.43; found C 46.63, H 4.62, N 5.36. IR (KBr): $\tilde{\nu}$ = 3425 (m) [νO–H(water)]; 1622 (s) [ν(C=N)]; 1090 (vs), 621 (w) [$\nu(ClO_4)$] $\mathrm{cm^{-1}}$. μ_{eff} = 5.01 BM.

6: Red crystals. Yield: 85%. $C_{60}H_{72}Cl_2MnN_6Ni_3O_{23}$ (1547.23): calcd. C 46.58, H 4.69, N 5.43; found C 46.65, H 4.71, N 5.48. IR (KBr): $\tilde{\nu}$ = 3411 (w) [νO–H(water)]; 1621(vs) [ν(C=N)]; 1090 (vs), 622 (w) [$\nu(ClO_4)$] $\mathrm{cm^{-1}}$. μ_{eff} = 5.84 BM.

Crystal-Structure Determination of 1–6: Single-crystal X-ray intensity data of the title compounds were collected with the following diffractometer types, all of which employed graphite-monochromated Mo-K_α radiation (λ = 0.71073 Å) and CCD area detectors: Bruker AXS SMART (compound **1**), Bruker-APEX II SMART CCD (compound **2**), Bruker-Nonius Kappa (compounds **3** and **6**) and Bruker-Nonius APEX II (compounds **4** and **5**).

The intensity data were processed with the program suites DENZO-SMN,[13a] Bruker SMART,[13b] SAINT[13b] and SADABS,[13c] and corrected for Lorentz, polarization, background and absorption effects.[13d] The orthorhombic crystal system and the *Pbcn* space group were selected for **1**. The crystal system for compounds **2**–**6** is monoclinic and the space group is *C*2/*c*. The crystal structures were determined by direct methods and subsequent Fourier and difference Fourier syntheses, followed by full-matrix least-squares refinements on F^2.[13e] Scattering factors for neutral atoms were employed in the refinements.

The hydrogen atoms of the water molecule of **1**, both the water molecules of **6** and one of the two water molecules of **4** were located from the difference Fourier maps, whereas the hydrogen atoms of the second water molecule in **4** and both the two water molecules in **2**, **3** and **5** were not located and therefore were not considered in the refinement process. For structures **1**–**6**, other hydrogen atoms were inserted at geometrical calculated positions with fixed thermal parameters. All non-hydrogen atoms were refined anisotropically and all hydrogen atoms isotropically. One problem observed in the refinement was the displacement parameters of the terminal ethyl groups. Another problem observed was the disorder of water oxygen atom O(2) in **2**–**6**. However, attempts to model these disorders were not successful; all these models did not yield better agreement than the structure presented here. Because there are no interactions between these groups and neighbouring units, the displacement did not converge on a final value but kept on changing regardless of the number of refinement cycles. However, because these up-and-down shifts are neither large nor in any way relevant for the significant structural aspects (water inclusion and cocrystallization) discussed in this paper, this does not present a problem. The final R_1 values of the refinements were 0.023, 0.058, 0.083, 0.046, 0.058 and 0.043, respectively, for **1**, **2**, **3**, **4**, **5** and **6**. Essential crystallographic information is listed in Table 3.

It may be mentioned that the structures of **2**–**6** can also be reasonably refined in the noncentrosymmetric space group *Cc*. However, Platon check on *Cc* cif files suggests centrosymmetric space group and therefore the *C*2/*c* space group was selected. The R_1 values of the refinement in two space groups are compared in Table S2 (Supporting Information).

CCDC-603249 (for **1**), -740024, -715229, -715230, -715231 and -715232 (for **2**–**6**, respectively, having space group *C*2/*c*), and -720139, -740020, -740021, -740022 and -740023 (for **2**–**6**, respectively, having space group *Cc*) contain the supplementary crystallographic data for this paper. These data can be obtained free of charge from The Cambridge Crystallographic Data Centre via www.ccdc.cam.ac.uk/data_request/cif.

Supporting Information (see footnote on the first page of this article): Selected bond lengths and angles of the NiN_2O_2 coordination environment in **2**−**6**; comparison of the R_1 values of **2**−**6** refined in the *C*2/*c* and *Cc* space groups; crystal structures of **3**–**5**; MS (ESI+) of **3** and **4**.

Table 3. Crystallographic information for **1**–**6**.

	1	**2**	**3**	**4**	**5**	**6**
Formula	$C_{20}H_{24}N_2O_5Ni$	$C_{60}H_{72}N_6\ O_{23}Cl_2Ni_3Cu$	$C_{60}H_{72}N_6O_{23}Cl_2Ni_4$	$C_{60}H_{72}N_6O_{23}Cl_2Ni_3Co$	$C_{60}H_{72}N_6O_{23}Cl_2Ni_3Fe$	$C_{60}H_{72}N_6O_{23}Cl_2Ni_3Mn$
Formula weight	431.12	1555.81	1550.98	1551.20	1548.12	1547.21
Crystal system	orthorhombic	monoclinic	monoclinic	monoclinic	monoclinic	monoclinic
Space group	*Pbcn*	*C*2/*c*	*C*2/*c*	*C*2/*c*	*C*2/*c*	*C*2/*c*
a / Å	12.7783(17)	15.4488(14)	15.4875(4)	15.4584(10)	15.4392(4)	15.4374(2)
b / Å	19.344(3)	22.2418(19)	22.3998(6)	22.4523(10)	22.4137(5)	22.4444(3)
c / Å	7.5097(10)	18.4228(17)	18.7001(6)	18.7995(10)	18.7787(4)	18.8553(3)
β / °	90.00	95.149(2)	94.287(2)	94.596(3)	94.3220(10)	94.6810(10)
V / Å^3	1856.3(4)	6304.7(10)	6469.2(3)	6503.9(6)	6479.9(3)	6511.25(16)
Z	4	4	4	4	4	4
T / K	120(2)	120(2)	293(2)	293(2)	293(2)	293(2)
R_1[a]/wR_2[b] [for $F_o > 4\sigma(F_o)$]	0.0234/ 0.0698	0.0585/ 0.1514	0.0832/ 0.2392	0.0464/ 0.1248	0.0582/ 0.1583	0.0427/ 0.1061
R_1[a]/wR_2[b] (for all F_o^2)	0.0253/ 0.0714	0.1181/ 0.1838	0.0949/ 0.2482	0.0532/ 0.1321	0.1193/ 0.1881	0.0655/ 0.1176

[a] $R_1 = [\Sigma||F_o| - |F_c||/\Sigma|F_o|]$. [b] $wR_2 = [\Sigma w(F_o^2 - F_c^2)^2/\Sigma w(F_o^2)^2]^{1/2}$.

Acknowledgments

Financial support from the Department of Science and Technology, the Government of India (SR/S1/IC-12/2008) is gratefully acknowledged. R. K. thanks the Centre for Research in Nanoscience and Nanotechnology, University of Calcutta, S. S. thanks the University Grants Commission (UGC), Government of India and S. D. thanks the Council of Scientific and Industrial Research (CSIR), Government of India, for providing fellowships.

---

[1] a) R. Robson in *Comprehensive Supramolecular Chemistry* (Eds.: J. L. Atwood , J. E. D. Davies, D. D. MacNicol, F. Vögtle, R. B. Toda), Pergamon, Oxford, **1996**, vol. 6, pp. 733–755; b) A. J. Blake, N. R. Champness, P. Hubberstey, M. A. Withersby, M. Schröder, *Coord. Chem. Rev.* **1999**, *183*, 117; c) J.-P. Sauvage (Ed.), *Transition Metals in Supramolecular Chemistry (Perspectives in Supramolecular Chemistry)*, Wiley, England, **1999**, vol. 5; d) G. R. Desiraju (Ed.), *The Crystal as a Supramolecular Entity (Perspectives in Supramolecular Chemistry)*, Wiley, England, **1996**, vol. 2; e) D. Braga, F. Grepioni, A. G. Orpen, *Crystal Engineering: from Molecules and Crystals to Materials*, Kluwer Academic, Dordrecht, **1999**; f) D. Braga, L. Maini, M. Polito, L. Scaccianoce, G. Cojazzi, F. Grepioni, *Coord. Chem. Rev.* **2001**, *216*, 225; g) B. Moulton, M. J. Zaworotko, *Chem. Rev.* **2001**, *101*, 1629.

[2] a) G. J. McManus, J. J. Perry IV, M. Perry, M. Perry, B. D. Wagner, M. J. Zaworotko, *J. Am. Chem. Soc.* **2007**, *129*, 9094; b) M. R. Marvel, J. Lesage, J. Baek, P. S. Halasyamani, C. L. Stern, K. R. Poeppelmeier, *J. Am. Chem. Soc.* **2007**, *129*, 13963; c) F. Nouar, J. F. Eubank, T. Bousquet, L. Wojtas, M. J. Zaworotko, M. Eddaoudi, *J. Am. Chem. Soc.* **2008**, *130*, 1833; d) K. Uemura, K. Saito, S. Kitagawa, H. Kita, *J. Am. Chem. Soc.* **2006**, *128*, 16122; e) A. R. Millward, O. M. Yaghi, *J. Am. Chem. Soc.* **2005**, *127*, 17998; f) J. L. C. Rowsell, O. M. Yaghi, *J. Am. Chem. Soc.* **2006**, *128*, 1304.

[3] a) M. Nayak, R. Koner, H.-H. Lin, U. Flörke, H.-H. Wei, S. Mohanta, *Inorg. Chem.* **2006**, *45*, 10764; b) M. Nayak, S. Hazra, P. Lemoine, R. Koner, C. R. Lucas, S. Mohanta, *Polyhedron* **2008**, *27*, 1201; c) M. Fleck, S. Hazra, S. Majumder, S. Mohanta, *Cryst. Res. Technol.* **2008**, *43*, 1220.

[4] a) H. Koshima, M. Nagano, T. Asahi, *J. Am. Chem. Soc.* **2005**, *127*, 2455; b) S. L. Childs, L. J. Chyall, J. T. Dunlap, V. N. Smolenskaya, B. C. Stahly, G. P. Stahly, *J. Am. Chem. Soc.* **2004**, *126*, 13335; c) J. F. Remenar, S. L. Morissette, M. L. Peterson, B. Moulton, J. M. MacPhee, H. R. Guzman, O. Almarsson, *J. Am. Chem. Soc.* **2003**, *125*, 8456; d) X.-L. Zhang, X.-M. Chen, *Cryst. Growth Des.* **2005**, *5*, 617.

[5] a) T. E. Keyes, R. J. Forster, A. M. Bond, W. Miao, *J. Am. Chem. Soc.* **2001**, *123*, 2877; b) U. Geiser, S. K. Kumar, B. M. Savall, S. S. Harried, K. D. Carlson, P. R. Mobley, H.-H. Wang, J. M. Williams, R. E. Botto, *Chem. Mater.* **1992**, *4*, 1077; c) B. Olenik, R. Boese, R. Sustmann, *Cryst. Growth Des.* **2003**, *3*, 175; d) F. Pan, M. S. Wong, V. Gramlich, C. Bosshard, P. Gunter, *J. Am. Chem. Soc.* **1996**, *118*, 6315.

[6] a) H. Koshima, H. Miyamoto, I. Yagi, K. Uosaki, *Cryst. Growth Des.* **2004**, *4*, 807; b) S. Ohba, H. Hosomi, Y. Ito, *J. Am. Chem. Soc.* **2001**, *123*, 6349; c) J. H. Loehlin, M. C. Etter, C. Gendreau, E. E. Cervasio, *Chem. Mater.* **1994**, *6*, 1218; d) B. R. Bhogala, A. Nangia, *Cryst. Growth Des.* **2003**, *3*, 547.

[7] a) H. M. Lee, M. M. Olmstead, G. G. Gross, A. L. Balch, *Cryst. Growth Des.* **2003**, *3*, 691; b) M. M. Olmstead, P. Wei, A. S. Ginwalla, A. L. Balch, *Inorg. Chem.* **2000**, *39*, 4555; c) P. Le Magueres, S. M. Hubig, S. V. Lindeman, P. Veya, J. K. Kochi, *J. Am. Chem. Soc.* **2000**, *122*, 10073; d) I. Ara, J. Fornies, J. Gomez, E. Lalinde, M. T. Moreno, *Organometallics* **2000**, *19*, 3137.

[8] a) C.-C. Chou, C.-C. Su, H.-L. Tsai, K.-H. Lii, *Inorg. Chem.* **2005**, *44*, 628; b) M. Palaniandavar, R. J. Butcher, A. W. Addison, *Inorg. Chem.* **1996**, *35*, 467; c) R. C. Holz, L. C. Thompson, *Inorg. Chem.* **1993**, *32*, 5251; d) P. Jones, R. S. Vagg, P. A. Williams, *Inorg. Chem.* **1984**, *23*, 4110; e) W. J. Evans, T. J. Boyle, J. W. Ziller, *Inorg. Chem.* **1992**, *31*, 1120.

[9] a) R. Koner, H.-H. Lin, H. H. Wei, S. Mohanta, *Inorg. Chem.* **2005**, *44*, 3524; b) R. Koner, G.-H. Lee, Y. Wang, H.-H. Wei, S. Mohanta, *Eur. J. Inorg. Chem.* **2005**, 1500.

[10] a) G. Hoshina, M. Tsuchimoto, S. Ohba, *Bull. Chem. Soc. Jpn.* **2000**, *73*, 369; b) D. Cunningham, J. F. Gallagher, T. Higgins, P. McArdle, J. McGinley, M. O'Gara, *J. Chem. Soc., Dalton Trans.* **1993**, 2183; c) J. R. Zamian, E. R. Dockal, G. Castellano, G. Oliva, *Polyhedron* **1995**, *14*, 2411.

[11] The Cambridge Structural Database (*CSD*), Version 5.30, **2008**.

[12] S. Mohanta et al., manuscript in preparation.

[13] a) *Bruker-Nonius: COLLECT*, Nonius, Delft, The Netherlands, **2003**; b) *Bruker-Nonius, APEX-II and SAINT-Plus*, Bruker AXS Inc., Madison, Wisconsin, USA, **2004**; c) C. H. Görbitz, *Acta Crystallogr., Sect. B* **1999**, *55*, 1090; d) G. M. Sheldrick, *Acta Crystallogr., Sect. A* **2008**, *64*, 112; e) processing of X-ray diffraction data collected in oscillation mode. Z. Otwinowski, W. Minor, *Methods Enzymol.* **1997**, *276*, 307; f) A. L. Spek, *J. Appl. Crystallogr.* **2003**, *36*, 7.

Received: July 21, 2009